

EVALUATING THE RELATIONSHIP BETWEEN ELECTROLUMINESCENCE (EL) IMAGING AND THE POWER OUTPUT OF PHOTOVOLTAIC MODULES

Crozier J.L.*, van Dyk E.E. and Vorster F.J.

*Author for correspondence

Department of Physics,
Nelson Mandela Metropolitan University,
Port Elizabeth, 6031,
South Africa

Email: s207094248@live.nmmu.ac.za;

ABSTRACT

Electroluminescence (EL) is a useful solar cell and photovoltaic module characterisation technique as it is fast, non-destructive and sensitive to the effects of shunt and series resistance and recombination processes. EL is emitted by a solar cell under forward bias, as injected carriers recombine radiatively and can be detected by a cooled silicon CCD camera in dark conditions or with appropriate optical filters. There is a relationship between the localised intensity of the emitted EL and the corresponding photo-response of the cell at a point [1-3]. Thus EL imaging allows cracks, breaks and defects to be identified. These defects can have a significant effect of the performance and longevity of the module. Cracks result in inactive areas which limit the current generated by the cell. Cells are connected in series in a module so the power output of the entire module is affected. This study investigates the relationship between the EL image of observed features and the power output of the module. It is shown that the extent to which the power and current of a module are affected by cell fractures depends on the area and position of the fracture. Other features such broken contact fingers and small micro-cracks are observed to have a minimal effect on the power output.

INTRODUCTION

The current-voltage (I-V) characteristics of a solar cell are represented by a diode equation and an equivalent circuit which successfully describes the electrical behaviour of a solar cell [4]. The I-V characteristics of a solar cell or module can be measured using an indoor solar simulator or an outdoor current-voltage measurement system. The illuminated I-V curve occurs in the fourth quadrant, however, the convention is to use the absolute value of current and thus reflect the curve in the first quadrant [5]. In the I-V curve the power output of the cell is at a maximum when the product of current and voltage is at a maximum. The I_{MAX} and V_{MAX} are the current and voltage points that correspond to the maximum power point, P_{MAX} .

The Standard Test Conditions (STC) are 1000 W/m^2 and 25° C . The temperature and irradiance conditions at the time of measurement influence the shape of the I-V curve. Measurements should be taken at irradiance values greater than 700 W/m^2 , thereafter the current is corrected to an irradiance of 1000 W/m^2 . The accuracy of the temperature and irradiance measurements affects the uncertainty of the final power measurement as corrections to STC are performed.

The short circuit current (I_{SC}) is the current value that occurs when the voltage is zero. The I_{SC} is equivalent to the photogenerated current (I_{PH}) unless the series resistance is high and there is a significant amount of leakage current flowing through the shunt resistance [4]. The open circuit voltage (V_{OC})

is a measure of the strength of the bias that occurs over the junction due to the photogenerated carriers [5]. The fill factor (FF) is the ratio of the maximum power output to the product of short circuit current and open circuit voltage. Fill factor gives an indication of how the shape of the I-V curve varies from the ideal shape due to the effects of series and shunt resistances.

In real solar cells series resistance occurs due to resistances along the current path to the external circuit of the collected carrier [4]. The series resistance includes the resistance in the bulk of the material, the emitter, the contacts and busbars. The presence of series resistance limits the current output and causes a drop in voltage at a specific current which lowers the fill factor of the curve [6]. Increasing the series resistance results in the I-V characteristic becoming flattened at the “knee” and at high series resistances the curve resembles the ohmic behaviour of a resistor.

A deviation in the I-V curve between the measured curve and the ideal curve can be indicative of various defects which are discussed:

- i. **Lower Short-circuit current (I_{sc}):** The current of module is linked to the illumination levels. Lower illumination levels or uniform shading decreases the current output of the module [7]. This can also be caused by degradation and discolouration in the

- encapsulant layers. Alternatively if cells in multiple strings are equally degraded or damaged there will be a decrease in I_{SC} and the I-V curve will not have steps.
- ii. **Lower Open-circuit voltage (V_{OC}):** The V_{OC} of a module is equal to the sum of the voltages of each cell connected in series. Lower than expected V_{OC} can be attributed to shunts over the cell, where the interconnections are faulty or there is a faulty bypass diode. Alternatively, since V_{OC} is highly temperature dependant, inaccuracy in the temperature measurements and corrections can result in lower or higher than expected V_{OC} . Potential-Induced Degradation (PID) also reduces the V_{OC} of the module.
 - iii. **Steps in I-V Curve:** Steps in the bypass diodes are attributed to a mismatch in the current in strings which activates the bypass diode[6]. Cracks or defects occurring in a localised area of the module will result in steps in the I-V curve corresponding with the activation of bypass diodes.
 - iv. **Gradient of slope near I_{SC} :** The low voltage region of the curve close to I_{SC} is affected by shunt resistance. If the shunt resistance decreases due to the presence of shunting over cells in the module the slope in this region will be steeper.
 - v. **Gradient of slope near V_{OC} :** This region of the I-V curve is affected by series resistance. Poor interconnection, contacts or junction box can result in the slope from V_{OC} to the “knee” becoming steeper.

ELECTROLUMINESCENCE (EL)

Electroluminescence (EL) is a non-destructive characterisation technique that allows defects and features in solar cells to be quickly identified. A solar cell or module is forward biased and the radiative recombination of injected carriers results in photons emitted from the surface of the cell. The intensity of the emitted luminescence is dependent on the optical, electrical and resistive properties of the solar cell. The EL is strongly dependant on the applied bias conditions and increased applied bias results in increased EL intensity and thus areas of high series resistances result in decreased EL intensity. EL imaging is very effective in detecting defects in modules such as cracks, broken fingers and broken cells[8]. For this reason it is extensively integrated into module production lines and module testing systems and highlights features that are missed during visual inspection[9]. The EL images can be quantitatively assessed in order to determine the resistive and recombination properties [1, 2, 7].

Silicon solar cells are made of thin, fragile wafers making the occurrence of micro-cracks fairly common if cells and modules are not handled correctly. Micro-cracks can occur in the manufacturing process of the cells and modules or in the transport, handling and installation of the module. While severe cracks can be detected using an optical microscope, micro-cracks will not be visible and this is a time consuming process. EL provides a quick way of identifying cracks in cells and modules. Micro-cracks appear in EL images as dark lines and the position and orientation of the cracks can be indicative of their cause[10].

In mono-crystalline silicon cells they are easily identified but in multi-crystalline silicon cells it can be hard to distinguish them from the dark lines and shapes of the crystal inhomogeneities and grain boundaries. The effect of these cracks on the module power output depends on the extent of the cracks and whether the cracks remove portions of the cells from electrical contact[10]. Micro-cracks have also been shown to lower short-circuit current and efficiency while increasing recombination current [11]. A crack in the cell material prevents electrical contact to the area and either fewer minority charge carriers are generated or none at all. The lack of radiative recombination in these areas renders these defects visible in the EL image.

The classification of micro-cracks is discussed by Köntges et al [12] and divided into 3 classes:

- i. **Class A:** Micro-cracks are visible in the EL but do not cause inactive areas of the cell. The crack does not affect current flow and thus the EL intensity is roughly equivalent on either sides of the crack.
- ii. **Class B:** Micro-cracks result in an area of the cell that is darker in the EL image but that is still connected in the cell.
- iii. **Class C:** Micro-cracks completely remove areas of the cell from electrical contact which appear completely dark in the EL image.

The effect on the power output of class A micro-cracks is minimal but has been shown that with time and thermal cycling class A micro-cracks can develop into B or C micro-cracks[12].

EXPERIMENTAL PROCEDURE

Five mono-crystalline modules are tested pre-exposure. These modules all have the same specifications and dimensions. The modules are rated at $P_{MAX} = 85W$, $V_{OC} = 44.0V$ and $I_{SC} = 2.61A$. They consist of 72 cells each with an area of 12.4 x 5.6 cm. The I-V curve is measured using a class AAA indoor solar simulator where the irradiance and temperature corrections are performed. The correction procedure is followed in accordance with standard IEC 60904. The back of module temperature of the test module and the reference cell is measured and the temperature corrections are made to the voltage and current using the manufacturers' supplied temperature coefficient. The irradiance is measured using a calibrated reference cell and the measured current is corrected to 1000W/m². The performance parameters (P_{MAX} , V_{OC} , FF and I_{SC}) are extracted from the corrected curve. EL images of the module are recorded using a cooled-CCD camera with appropriate filters. The camera setup is optimised for the bulk testing of modules so that image resolution is sacrificed so that the EL test can be integrated into the module testing production line.

RESULTS

The I-V curve of each module is plotted in figure 1, these curves have been corrected to Standard Test Conditions, 25°C and 1000 W/m². Modules 1 to 4 have typical I-V curves without steps and with normal slopes near I_{SC} and V_{OC} . Module 5 has a step in the I-V curve indicating the activation of

the bypass diode across the string due to current mismatch between the strings.

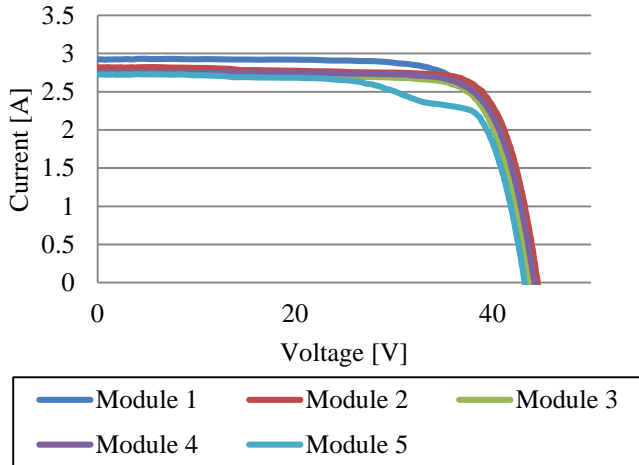


Figure 1 The I-V curve of the test modules corrected to STC. Module 5 shows the steps in the I-V curve indicating the activation of a bypass diode and cell mismatch.

The maximum power point of each module is extracted from the I-V curves and is plotted in figure 2. Modules 1-4 have exceeded the rated power and have a P_{MAX} of between 94-99 W. Module 5 has considerably lower P_{MAX} than the other modules, however it still is in the $\pm 3\%$ tolerance region for an 85 W module. The uncertainty in the power measurement is 4%, indicated with error bars.

The I_{SC} of each module is plotted with error bars of 4% uncertainty in figure 3, the modules are all greater than the rated short-circuit current. Modules 3, 4 and 5 have about the same I_{SC} even though module 5 has a much lower power. This is because the bypass diodes in module 5 is activated, therefore increasing the I_{SC} . The V_{OC} of each module is plotted with error bars of 4% uncertainty in figure 4. The measured currents are all above the rated current and the voltages are all within the rated range. It is important that the voltage provided by a module is correctly specified as the maximum power point tracker, charge controller and inverter are not able to handle large variations in voltage. The Fill Factor for each curve is plotted in figure 4, where module 5 has the lowest FF owing to the steps in the I-V curve due to the activation of the bypass diode.

These modules have been underspecified and have a maximum power output greater than 85 W. This probably due to the manufacturer or distributor deciding that there is a greater market for 85W modules. Under specification would not be considered a problem for most applications provided the voltage is as specified.

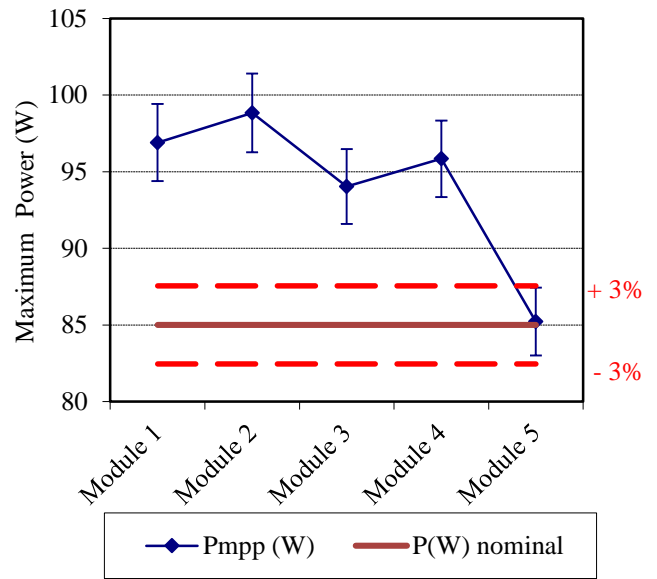


Figure 2 The maximum power of the tested modules compared to the rated power. The modules are underrated by about 10 W so all except one greatly exceed the rated power. Module 5 falls within the rated power range.

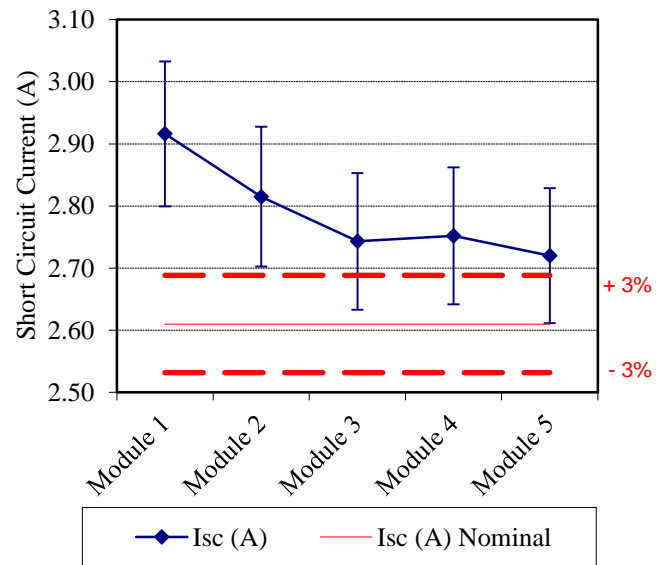


Figure 3 The short-circuit current of the test modules compared with their rated current.

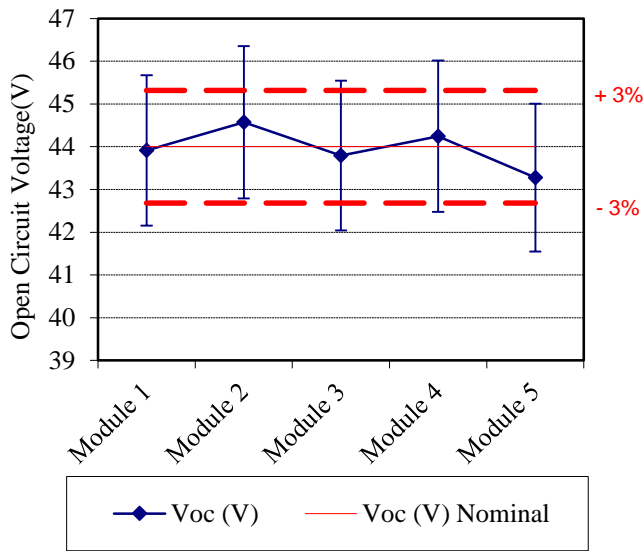


Figure 4 The open-circuit voltage of the test modules compared with their rated voltage.

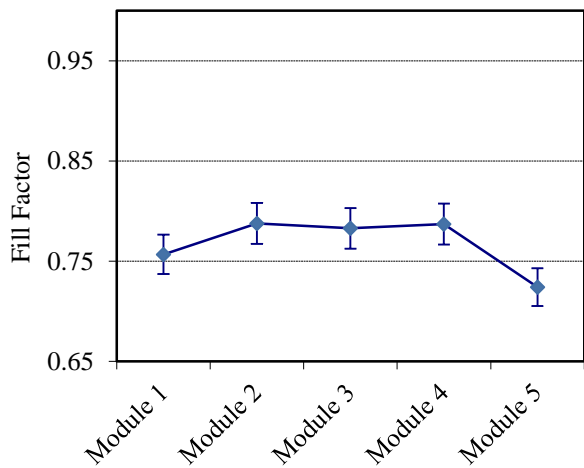


Figure 5 The Fill factor of the test modules.

The EL images of the 5 modules are shown in figure 6. Some of the cells with defects are highlighted in the image in order to indicate which EL features correspond with which defects. The results of the test are summarised as follows:

Module 1: No severe defects, some broken finger contacts which result in darker areas on the cells.

Module 2: Micro-cracks in a several cells, broken finger contacts and poor cell interconnection.

Module 3: Micro-cracks, broken finger contacts.

Module 4: Micro-cracks

Module 5: “Tyre Tracks” due to contact forming failures, broken finger contacts, poor cell interconnection and micro-cracks.

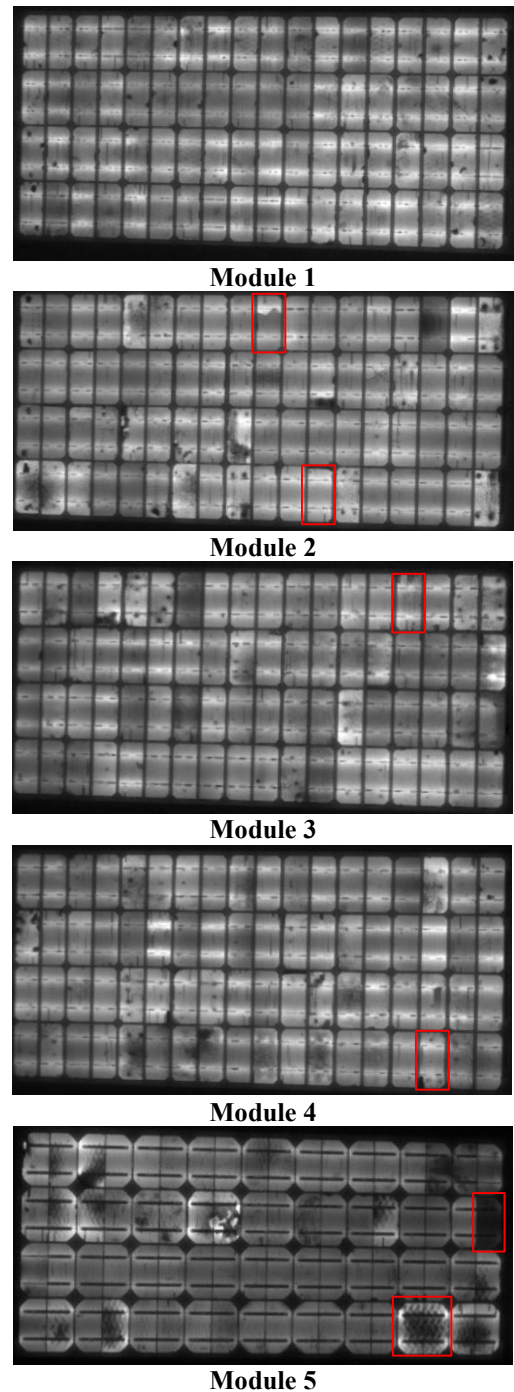


Figure 6 The EL image of test modules taken at an applied forward current equal to I_{SC} . The pixel size is approximately 2 mm. The low resolution of the image can make defects more difficult to determine. The following examples of defects are highlighted: a) Module 2- A cell with a micro-crack running parallel to the busbars, b) Module 2- A cell with a broken contact finger, c) Module 3- a cell with broken fingers and a micro-crack, d) Module 4- A cell with a micro-crack, e) Module 5- Darker cell due to poor cell connection and f) Module 5- Cell with tyre track defect is highlighted.

As expected from the results of the I-V characterisation module 5 has many defects observed in the EL image. One cell appears much darker than the others indicating high series resistance in the busbars thus lowering the experienced applied bias and the cell appears darker than the other cells. The “tyre tracks” on many of the cells occur due to temperature inhomogeneities that occur during the metallisation process of the cells. These features are commonly observed in crystalline silicon solar cell and do not significantly lower the current of the affected cells[13]. Tyre tracks occur during the manufacturing process so their presence in only module 5 points to a different manufacturing batch, supported by the slightly different appearance of module 5 in the EL image. There are also micro-cracks that contribute to lower current. As the micro-cracks and poorly contacted cell occur in the same string (the top two rows of cells in figure 6) the bypass diode is activated over that string which results in the step in the I-V curve that is observed in figure 1. Module 1 does not have any severe defects which explains the higher current observed in figure 3, compared with the other modules.

CONCLUSION

This study discussed the I-V curve and the performance parameters of five PV modules. A drop in each parameter indicates a potential defect or failure in the module. Module 5 has a lower than average power and fill factor which is attributed to cell mismatch since there is a step in the I-V curve. The presence of micro-cracks and poorly connected cells is confirmed by the EL image.

The I-V curve and performance parameters are usually used to identify failure modules and they are able to give an indication of the possible causes of the lower parameters. However, the EL image provides a clearer idea of the defects that are present. Many features observed in an EL image will not significantly affect the module performance so it is important to employ both techniques to completely characterise the module.

REFERENCES

1. Rau, U., *Reciprocity relation between photovoltaic quantum efficiency and electroluminescent emission of solar cells*. Physical Review B, 2007. **76**(8).
2. Würfel, P., et al., *Diffusion lengths of silicon solar cells from luminescence images*. Journal of Applied Physics, 2007. **101**(12): p. 123110.
3. Kirchartz, T., et al., *Reciprocity between electroluminescence and quantum efficiency used for the characterization of silicon solar cells*. Progress in Photovoltaics: Research and Applications, 2009. **17**(6): p. 394-402.
4. Overstraeten, R.J. and R.P. Mertens, *Physics, Technology and Use of Photovoltaics*. 1986, Bristol: Adam Helger.

5. Mazer, J.A., *Solar Cells: An Introduction to Crystalline Photovoltaic Technology*. 1996, Boston: Kluwer Academic Pub.
6. Crozier, J.L., *Characterization of cell mismatch in photovoltaic modules using electroluminescence and associated electro-optic techniques*, in *Physics2012*, Nelson Mandela Metropolitan University: Port Elizabeth.
7. Häberlin, H., *Photovoltaics: System Design and Practice*. 2012, Chichester, West Sussex, UK: John Wiley & Sons Ltd.
8. Mansouri, A., et al. *Defect detection in photovoltaic modules using electroluminescence imaging*. in *27th European Photovoltaic Solar Energy Conference and Exhibition*. 2012. Frankfurt, Germany.
9. Camino-Villacorta, M., et al. *Comparative Analysis of Electroluminescence, IR Thermography and Visual Inspection on c-Si Modules*. in *27th European Photovoltaic Solar Energy Conference and Exhibition*. 2012. Frankfurt, Germany.
10. Kajari-Schröder, S., et al., *Spatial and orientational distribution of cracks in crystalline photovoltaic modules generated by mechanical load tests*. Solar Energy Materials and Solar Cells, 2011. **95**(11): p. 3054-3059.
11. van Mülken, J.I., et al., *Impact of Micro-Cracks on the Degradation of Solar Cell Performance Based On Two-Diode Model Parameters*. Energy Procedia, 2012. **27**: p. 167-172.
12. Köntges, M., et al., *The risk of power loss in crystalline silicon based photovoltaic modules due to micro-cracks*. Solar Energy Materials and Solar Cells, 2011. **95**(4): p. 1131-1137.
13. IEAPVPS, *Performance and Reliability of Photovoltaic Systems Subtask 3.2:Review of Failures of Photovoltaic Modules*, 2014, IEA International Energy Agency.